Journal of Power Sources 293 (2015) 846–851

Contents lists available at ScienceDirect

Journal of Power Sources

journal homepage: www.elsevier.com/locate/jpowsour

Multilayer graphene for long-term corrosion protection of stainless steel bipolar plates for polymer electrolyte membrane fuel cell

Adam C. Stoot [a], Luca Camilli [a], Susie-Ann Spiegelhauer [b], Feng Yu [a], Peter Bøggild [a, *]

[a] Technical University of Denmark, Department of Micro- and Nanotechnology, Kgs. Lyngby, DK-2800, Denmark
[b] Accoat, SP-Group A/S, Kvistgård, DK-3490, Denmark

HIGHLIGHTS

- Nickel-coating on stainless steel enhances its short term anti-corrosion properties.
- Multi-layer graphene film on steel enhances long-term corrosion resistance.
- The effect of nickel in corrosion resistance of graphene/nickel/steel is important.
- Accelerated reaction kinetics are used to simulate effect of longer exposures.

GRAPHICAL ABSTRACT

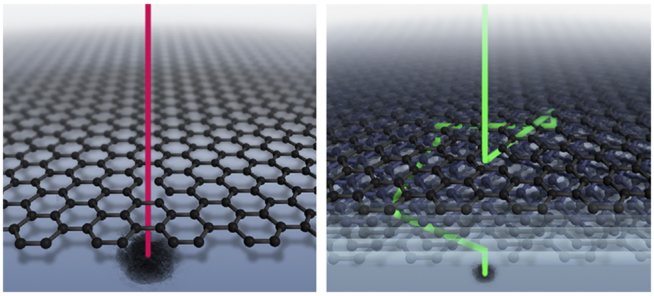

ARTICLE INFO

Article history:
Received 24 March 2015
Received in revised form
15 May 2015
Accepted 2 June 2015
Available online xxx

Keywords:
Graphene coating
Wet corrosion
Chemical vapour deposition
Raman spectroscopy
Stainless steel
Metal bipolar plate

ABSTRACT

Motivated by similar investigations recently published (Pu et al., 2015), we report a comparative corrosion study of three sets of samples relevant as bipolar plates for polymer electrolyte fuel cells: stainless steel, stainless steel with a nickel seed layer (Ni/SS) and stainless steel with Ni seed layer coated by a multi-layered graphene thin film (G/Ni/SS). The graphene film, synthesized by chemical vapour deposition (CVD), has a moderate amount of defects according to Raman spectroscopy. Short/medium-term corrosion test shows no significant advantage of using G/Ni/SS rather than Ni/SS, both samples exhibiting a similar trend, thus questioning the short-term positive effect of graphene coatings. However, partial immersion in boiling seawater for three weeks reveals a clear superiority of the graphene coating with respect to steel just protected by Ni. After the test, the graphene film is still intact with unchanged defect density. Our results show that even non-perfect multilayer graphene films can considerably increase the lifetime of future-generation bipolar plates for fuel cells.

1. Introduction

After the seminal works by Novoselov and Geim [1], the superior material properties of graphene has fuelled an intense search for practical applications of this planar honeycomb structure of carbon atoms. Graphene and related materials (*i.e.*, other two-dimensional crystals) are expected to have a major impact in several technological fields in the near future [2]. While graphene is chemically inert and impermeable to even hydrogen [3], the effectiveness of graphene as a protective coating is still subject to debate and controversy. While several studies have reported pronounced short- and medium-term protection performance of graphene coatings [4–6], Schriver et al. pointed out that graphene may in fact eventually accelerate corrosion and oxidation of metals over longer periods of time [7].

Very recently, Pu et al. proposed the use of graphene on stainless steel as a high-performance anti-corrosion coating for polymer

---

* Corresponding author.
E-mail address: peter.boggild@nanotech.dtu.dk (P. Bøggild).

http://dx.doi.org/10.1016/j.jpowsour.2015.06.009

electrolyte membrane fuel cells bipolar plates [8]. As the growth of large-scale high-quality graphene directly on stainless steel (SS) has not yet been shown to be possible, the authors suggest using a nickel (Ni) seed layer on top of SS (Ni/SS) in order to catalyse the graphene growth. The authors then compare the anti-corrosion performance of three sets of specimens: (i) bare SS, (ii) graphene-coated SS and (iii) graphene-coated Ni/SS (G/Ni/SS). After repeating a potentiodynamic polarization test twenty times for each set of samples they conclude that while the corrosion rate of bare SS and graphene-coated SS increases by almost 50 and 15 times, respectively, the corrosion rate of G/Ni/SS remains almost constant. Since in the case of graphene-coated SS specimen the graphene coverage is non-uniform and incomplete, while for the G/Ni/SS the coverage is close to 100%, the conclusion is that the complete surface coverage of the graphene coating prevents wet corrosion of SS. However, the effect of the Ni seed layer on SS has been overlooked, although Nickel based coatings and alloys have already been proposed as corrosion-resistive bipolar plates in fuel cells [9,10]. Here, we report that both the Ni/SS and the G/Ni/SS exhibit a similar behaviour when subjected to twenty polarization scans under same experimental conditions (2-h test), and thus that a graphene coating does not give a significant contribution to the short-term corrosion resistance of steel. In the long term, however, there is indeed a positive effect of graphene; after 504 h of exposure to boiling seawater (Atlas cell test, see Experimental section for details), there is indeed a clear difference in SS protected by Ni with or without graphene.

2. Experimental

2.1. Fabrication of samples

2 inch diameter, 3 mm thick 304 stainless steel samples were glass blasted and sonicated for 20 min in Triton X before being pre-coated with a 150 μm nickel seed layer using a Technotrans electroplating system without any additives/brighteners.

The chemical vapour deposition (CVD) system used for graphene growth is based on a graphitic block heated by halogen light bulbs and a PID-temperature control. Before insertion into the CVD-chamber, the samples were sonicated in isopropanol and then rinsed in deionized water. As for the growth process, firstly the samples were kept at 850 °C in hydrogen atmosphere for 10 min after which a mixture of hydrogen (24 sccm) and acetylene (12 sccm) was injected for the graphene growth. The samples were cooled down at a fixed rate of 0.5 °C/s in low vacuum (base pressure around 10^{-1} mbar).

2.2. Electrochemical tests

The electrochemical tests were done using a platinum counter electrode, an Ag/AgCl reference electrode and a Quick WE working electrode holder [11] along with the Gamry Reference 3000 potentiostat. The scan rate was 5 mV/s, and 3.5 wt% NaCl solution was the chosen electrolyte. Twenty polarisation scans were performed on each sample and the open circuit potential was monitored to ensure stabilisation between each scan.

2.3. Atlas cell tests

The simulated seawater tests were also done in 3.5 wt% NaCl solution. These long term tests were done at Accoat A/S using an Atlas glass cell. It consists of a glass canister with a hole in both ends allowing two samples to be tested simultaneously (see Supplementary Materials). The samples are only partially immersed in the corrosive solution, thus testing both liquid- and vapour phase-induced corrosion. Heating the solution to the boiling point has two effects; reaction kinetics is accelerated and large temperature gradients arise over the samples with their backside being exposed to room temperature. This furthermore tests the tendency of the coating to delaminate due to condensation and bubble formation at the coating/sample-interface in case of a semi-permeable coating or poor adhesion.

It is worth noting that the corrosive environment at an elevated temperature of the Atlas test presents a scenario similar to a fuel cell in operation, including the temperature gradients due to the surroundings being at a lower temperature.

2.4. Characterisation

The structure and composition of the samples were investigated with Scanning Electron Microscopy and Energy Dispersive Spectroscopy using FEI Quanta 200 FEG and FEI Inspect. Focused Ion Beam milling was done using FEI Helios dual beam focused ion beam microscope. Raman spectra were obtained using a Thermo Scientific DXR confocal Raman Microscope with a 455 nm laser, 2 mW power and a spot-size of approximately 1 μm.

3. Results and discussion

Fig. 1(a) shows an averaged Raman spectrum recorded on several locations of the G/Ni/SS sample. The ratio of the intensities of the 2D-peak (~2750 cm^{-1}) to the G-peak (~1590 cm^{-1}) is ~0.26 ± 0.01, indicating the multi-layered character of the graphene film. The thickness was 25 nm–40 nm measured by SEM of Focused Ion Beam milled sections (see supplementary materials). The D-band, located at ~1370 cm^{-1}, indicates the presence of defects and structural imperfections in the graphene lattice, which could be related to the small size of polycrystalline graphene domains [12]. Additionally, the Raman map displayed in Fig. 1(b) shows the full coverage and high homogeneity of the multilayer graphene coating over a millimetre-sized area of the sample, confirming the well-known high catalytic activity of Ni towards the synthesis of graphene [13].

In Fig. 2(a) we report the results of a single polarization scan acquired for three sets of samples: (i) bare SS, (ii) Ni/SS and (iii) G/Ni/SS. For comparison, we report on the same graph the data for a G/Ni/SS sample taken from Ref. [8]. Firstly, observing the anodic part of the polarization curve for SS (black curve), it is possible to observe the passivation layer formation (red arrow) and its subsequent break-down (blue arrow). Such a passivating film reduces the conductivity of the surface due to the oxide phase, and thus results in being detrimental in view of applications as a bipolar plate for polymer electrolyte membrane fuel cell. Secondly, we can see that the G/Ni/SS sample of Ref. [8] (brown curve) is performing better than our G/Ni/SS sample (blue curve), with a lower corrosion rate indicated by the curve being located at a lower current density range. We explain the difference with respect to our data as due to the larger defect density in our graphene film compared with the one reported by Pu et al. [8], which can be seen by direct comparison of the Raman spectrum in Fig. 1(a) of this work and the one displayed in Fig. 1(a) of Ref. [8]. In fact, it is well established that ions (such as Cl^- ions), water and oxygen may diffuse through defects of graphene, like grain boundaries and cracks, until reaching the metal surface underneath the coating and beginning its corrosion [14]. Lastly, we want to point out that our Ni/SS sample (green curve) is showing similar performance to the G/Ni/SS sample in Ref. [8] and, therefore, better performance than our G/Ni/SS specimen. This finding is actually not surprising, due to the intrinsic strong corrosion resistance of nickel and nickel-based alloys [15,16].

In order to (i) investigate the medium-term behaviour of the